# Journal Pre-proofs

Single-atom nanozymes possessing robust multienzyme-mimetic catalytic properties for sensing of volatile alkaline gas

Guangchun Song, Xiaochun Zheng, Zedong Zhang, Marie-Laure Fauconnier, Cheng Li, Li Chen, Dequan Zhang

Please cite this article as: G. Song, X. Zheng, Z. Zhang, M-L. Fauconnier, C. Li, L. Chen, D. Zhang, Single-atom nanozymes possessing robust multienzyme-mimetic catalytic properties for sensing of volatile alkaline gas, *Chemical Engineering Journal* (2024), doi: https://doi.org/10.1016/j.cej.2024.156835

This is a PDF file of an article that has undergone enhancements after acceptance, such as the addition of a cover page and metadata, and formatting for readability, but it is not yet the definitive version of record. This version will undergo additional copyediting, typesetting and review before it is published in its final form, but we are providing this version to give early visibility of the article. Please note that, during the production process, errors may be discovered which could affect the content, and all legal disclaimers that apply to the journal pertain.

# Single-atom nanozymes possessing robust multienzyme-mimetic catalytic properties for sensing of volatile alkaline gas

*Guangchun Song[1,2], Xiaochun Zheng[1], Zedong Zhang[3], Marie-Laure Fauconnier[2], Cheng Li[1], Li Chen[1], Dequan Zhang[1]\**

[1] Institute of Food Science and Technology, Chinese Academy of Agricultural Sciences, Key Laboratory of Agro-products Quality and Safety Control in Storage and Transport Process, Ministry of Agriculture and Rural Affairs, Beijing 100193, China.

[2] Laboratory of Chemistry of Natural Molecules, Gembloux Agro-Bio Tech, University of Liege, Passage des déportés 2, B-5030, Gembloux, Belgium.

[3] Department of Chemistry, Tsinghua University, Beijing, 100084 China.

E-mail: dequan_zhang0118@126.com

**ABSTRACT**

Volatile alkaline gases (VAGs) emitted from various sources, such as the food or chemical industry, pose potential harm to the natural environment and human health. Therefore, the development of a real-time, rapid, and cost-effective detection method is crucial. In this study, the enzyme-like catalytic types and activities of four different metal-based single-atom enzymes (Ga, Cu, Mn, and Zn SAzymes) were selected and evaluated. Among them, Ga SAzyme exhibited the most promising catalytic properties. Furthermore, the multienzyme catalytic properties of Ga SAzyme were utilized for the detection of ammonia, and it was found that its peroxidase-like (POD-like) activity showed a strong affinity for ammonia ($K_m$ = 0.05 mM). This detection strategy demonstrated high sensitivity, with a limit of detection (LOD) of 3.0 mM in the linear range of 0.01 - 0.05 M and 7.0 mM in the linear range of 0.075 - 0.25 M. Additionally, the method was characterized by fast response time (15 s) and low cost ($0.035 per sample). The proposed method holds great potential for the detection of VAGs from various sources in the future.

**Keywords:** Single-atom nanozymes; Multienzyme-like; Nano-sensing detection; Volatile alkaline gas

## 1. Introduction

Volatile alkaline gases (VAGs) have potential harm to the environment and human health. They can be generated through various processes, such as meat spoilage[1-3], chemical usage[4, 5], and waste disposal[6]. Failing to promptly monitor VAGs can result in significant food resource waste and may also lead to respiratory issues, central nervous system disorders, and cancer-related diseases[7, 8]. Spectroscopic techniques[9], chromatographic techniques[10], and chemical sensing technologies[11-14] have been utilized for VAGs detection. However, these technologies also have drawbacks, including high costs, complicated operations, and poor stability. Therefore, it is necessary to develop an affordable, rapid, and portable method to detect VAGs. This approach would not only enable real-time monitoring of food spoilage during storge but also assist in detecting harmful VAGs in the environment, thereby ensuring food quality and safety while protecting human health. Ammonia, as a kind of operable and easily available volatile alkaline gas, is a reliable and representative for this work.

Single-atom nanozymes (SAzymes) are a type of nanozymes that utilize separate metal atoms as their active centers. They exhibit catalytic activities similar to natural enzymes, and it was reported that they can mimic the catalytic activity of peroxidase (POD-like)[15], oxidase (OXD-like)[16], catalase (CAT-like)[17], superoxide dismutase (SOD-like)[18], glutathione peroxidase ($GP_x$-like)[19], and phosphatase (PPA-like)[20]. SAzymes have been used in various fields because of their efficient multienzyme mimetic catalytic properties, strong stability, and tolerance to harsh experimental conditions[21, 22]. They have been utilized for the detection of pesticide residues[23], heavy metal ions[24], biological toxins[25], organic pollutants[26], microorganisms[27], and volatile organic compounds[28]. However, metal species and coordination structure of SAzymes significantly affect their enzyme-like catalytic properties[16, 29, 30]. Consequently, further research is necessary to explore the rational selection and effective application of S Azyems with high enzyme-like catalytic properties.

In this study, the multienzyme-like catalytic activities of four types of SAzymes (Ga, Cu, Mn, and Zn) were systematically verified by examining their POD-, OXD-,

CAT-, SOD-, GP$_x$-, and PPA-like catalytic activities. And the Ga SAzyme exhibits the best multienzyme-like catalytic properties and shows a preliminary response to ammonia. It observed that ammonia had the most significant impact on the POD-like activity of Ga SAzyme. Further, a rapid, sensitive, low-cost, and portable method for detecting ammonia have been developed. This method shows the prospect of practical applications in various fields that may generate VAGs. This study not only enhances the validation strategies for the multienzyme-like catalytic properties of SAzymes but also broadens their practical applications in the fields of rapid food detection and environmental monitoring (Scheme 1).
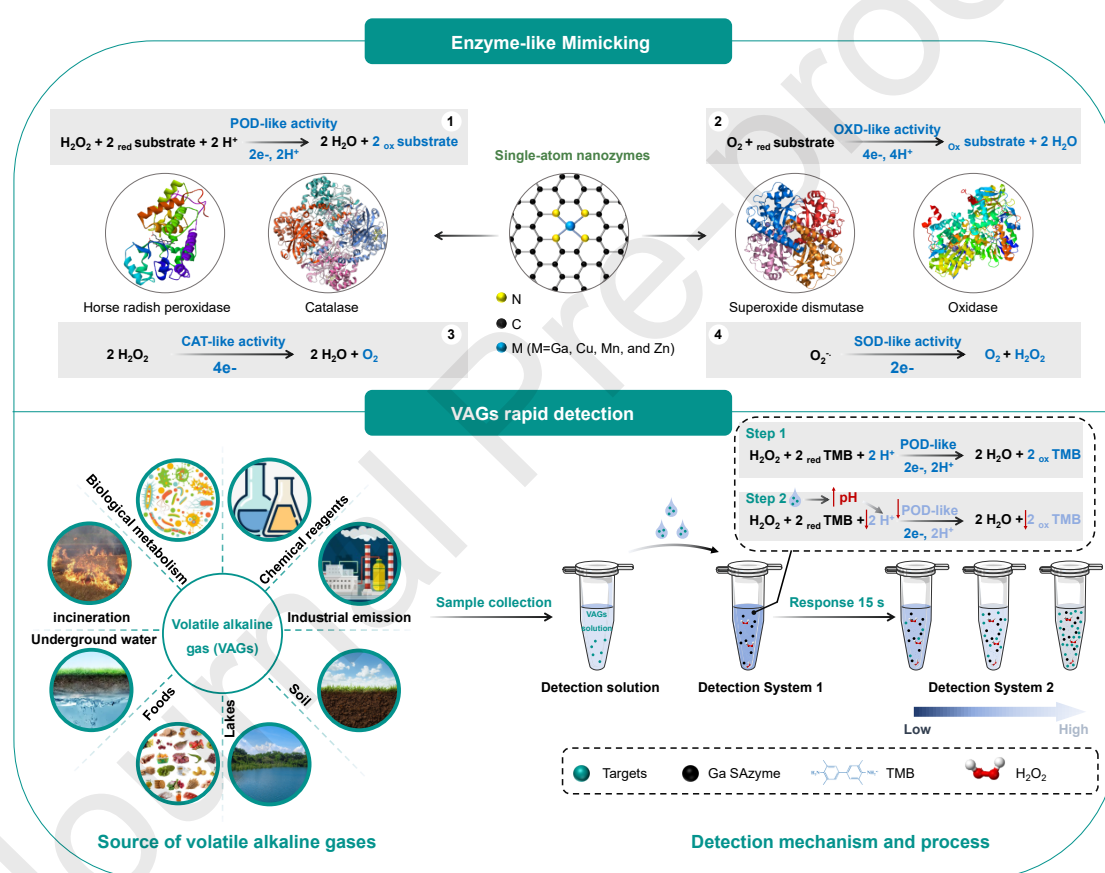


**Scheme 1.** Single-atom Ga nanozyme exhibits a stronger affinity for ammonia ($K_m$ = 0.05 mM) compared to TMB ($K_m$ = 0.07 mM). And a sensitive (LOD is 3.0 mM in the linear range of 0.01 - 0.05 M), rapid (15 s), and cost-effective ($0.035 per sample) detection method is developed for volatile alkaline gases.

## 2. Material and methods

### 2.1. Materials

Gallium nitrate anhydrous (Ga(NO$_3$)$_2$, analytical grade, 98%), copper nitrate

anhydrous (Cu(NO$_3$)$_2$, analytical grade, 98%), manganese (II) chloride tetrahydrate (MnCl$_2$·4H$_2$O, analytical grade, 98%), cupric chloride (CuCl$_2$, analytical grade, 98%), 2-methylimidazole (analytical grade, 98%), phosphonitrilic chloride trimer (analytical grade, 98%), bis(4-hydroxyphenyl) sulfone (analytical grade, 98%), bis(4-aminophenyl) ether (analytical grade, 98%) were purchased from Alfa Aesar. Zinc nitrate hexahydrate (Zn(NO$_3$)$_2$·6H$_2$O, analytical grade, 98%) was purchased from Bei Jing tongguang fine chemicals. Cyanuric chloride (analytical grade, 98%) was purchased from Tokyo Chemical Industry. Methanol (analytical grade) and N,N-dimethylformamide (analytical grade) were purchased from Sinopharm Chemical. Triethylamine (analytical grade) was purchased from Acros Organics. 3,3′,5,5′-Tetramethylbenzidine (TMB, analytical grade, 98%), 2,2′-azino-bis-(3-ethylbenzthiazoline-6-sulfonic acid) (ABTS, analytical grade, 98%), o-phenylenediamine (OPD, analytical grade, 98%), 10-Acetyl-3,7-dihydroxyphenoxazine (ADHP, analytical grade, 98%), dimethylamine, trimethylamine, and sodium hydrosulfide were purchased from Shanghai McLean Biochemical Technology Co., Ltd. Sodium acetate (NaHAc, analytical grade, 98%), and absolute ethanol (C$_2$H$_5$OH, analytical grade, 98%) were purchased from Shanghai Yuanye Biotechnology Co., Ltd. Glacial acetic acid (HAc, analytical grade, 98%) and horse radish peroxidase (analytical grade, 98%) were purchased from Beijing Hedder Technology Co. Ltd. Superoxide dismutase assay kit (analytical grade, 98%), glutathione peroxidase assay kit, and alkaline phosphatase assay kit were purchased from Shanghai Beyotime Biotechnology Technology Co., Ltd. Singlet oxygen ($^1$O$_2$) assay kit (BBoxiProbeẞ, green fluorescence, BB-47055, analytical grade, 98%), hydroxyl radical (•OH) assay kit (BBoxiProbeẞO28, red fluorescence, BB-46067, analytical grade, 98%), superoxide anion (O$_2$•$^-$) assay kit (BBoxiProbeẞO76, green fluorescence, BB-460622, analytical grade, 98%) were purchased from Shanghai Bestbio Biotechnology Co., Ltd.

2.2. Synthesis of single-atom nanozymes

To prepare Ga, Cu, Mn, and Zn SAzymes, 0.594 g of Zn(NO$_3$)$_2$·6H$_2$O and 37 mg of gallium / copper / manganese / zinc acetylacetonate (III) were dissolved in 10 mL

of methanol and sonicated to prepare solution A. Solution B was obtained by dissolving 0.656 g of 2-methylimidazole in 10 mL of methanol. Solution B was mixed with solution A and stirred for 3 mins. Furthermore, the mixed solution was transferred to a 50 mL Teflon reactor and heated at 120°C for 4 h in a constant temperature oven. The orange precipitate was collected by centrifugation, washed twice with methanol until the supernatant appeared colourless and transparent and then dried at 80°C. The Ga, Cu, Mn, and Zn SAzymes were produced by calcining the orange precipitate above at 950°C for 3 h under flowing nitrogen gas with a heating rate of 5°C min$^{-1}$[2, 31, 32].

## 2.3. Characterization of single-atom nanozymes

Transmission electron microscope (TEM) images of catalysts were collected with a FEI-Talos F200S TEM. High-angle annular dark-field scanning TEM (HAADF-STEM) images were recorded by a JEOL JEM-2100 F with an electron acceleration energy of 200 kV, which was equipped with a probe spherical aberration corrector. X-ray powder diffraction (XRD) spectra were obtained by using a Rigaku RU-200b x-ray diffractometer equipped with Cu Kα radiation (λ = 1.5406 Å). X-ray photoelectron spectroscopy (XPS) data were collected with ULVAC PHI Quantera. Inductively coupled plasma mass spectrometry (ICP-MS) data were collected with Agilent-7700.

## 2.4. Preparation of single-atom nanozymes solution

The Ga, Cu, Mn, and Zn SAzymes were each dissolved in ethanol and subjected to ultrasonic treatment. The concentration of each SAzyme stock solution was 70 μM.

## 2.5. Validation of enzyme-like catalytic activity

The POD-, OXD-, CAT-, SOD-, GP$_x$-, and PPA-like catalytic activities of Ga, Cu, Mn, and Zn SAzyme were verified, respectively. The detailed verification strategies are described in the supplementary information.

## 2.6. Optimization of enzyme-like reaction conditions

The absorbance values of Ga, Cu, Mn, and Zn SAzymes, as well as natural enzymes were recorded, at various pH values (pH 2, 4, 6, 8, and 12) and temperature values (-18, 4, 25, 35, 45, 55, 65, and 75°C), respectively.

2.7. Calculation of enzyme-like catalytic activity parameters

Under the optimal reaction conditions, the parameters for POD-, OXD-, and CAT-like catalytic activity can be calculated using the following procedures. The absorbance values were recorded at 10 s intervals over 400 seconds for different concentrations of TMB (0.025, 0.05, 0.1, 0.2, 0.4, 0.8, 1.6, 3.2, 6.4, 12.8, and 25.6 mM), $H_2O_2$ (0.0313, 0.0625, 0.125, 0.25, 0.375, 0.5, 0.625, 0.75, 0.875, 1, and 1.125 M), and SAzymes (0.9, 1.8, 2.7, 3.6, 4.5, 5.4, 6.3, 7.2, and 8.1 μM). The data was analyzed using the Michaelis-Menten equation to determine the values of the Michaelis constant ($K_m$), maximal reaction velocity ($v_{max}$), catalytic constant ($K_{cat}$), and specific activity (SA) parameters. The SA is defined as the enzyme-like activity in units per μmol of metal atom (Ga, Cu, Mn, and Zn).

2.8. Validation the species and contents of intermediate

Reactive oxygen species (e.g., •OH, $^1O_2$, and $O_2$•⁻) are products of catalytic reactions associated with enzyme-like activities. They were specifically identified and stained using confocal microscopy and quantitative analysis values were calculated by electron paramagnetic resonance (EPR) after 10 min. The confocal microscopy experiments were carried out according to the operational instructions of the hydroxyl radical assay kit, singlet oxygen assay kit, and superoxide anion assay kit. In addition to this, the specific recognition fluorescent probes for •OH, $^1O_2$, and $O_2$•⁻ were 5,5-dimethyl-1-pyrroline N-oxide (DMPO) and 2,2,6,6-Tetramethyl-1-piperidinyloxy (TEMP).

2.9. Application the optimal single-atom nanozyme for ammonia response

Ammonia was added to the optimal catalytic reaction system with POD-, OXD-, CAT-, and SOD-like activities. The visible colors and absorbance values of the four systems were observed and recorded using a UV-vis instrument. Based on the above results, the multienzyme-like activities with the greatest difference in absorbance values were determined. A sensitivity experiment was conducted within the ammonia concentration range of 0.01 to 0.25 M.

**3. Results and discussion**

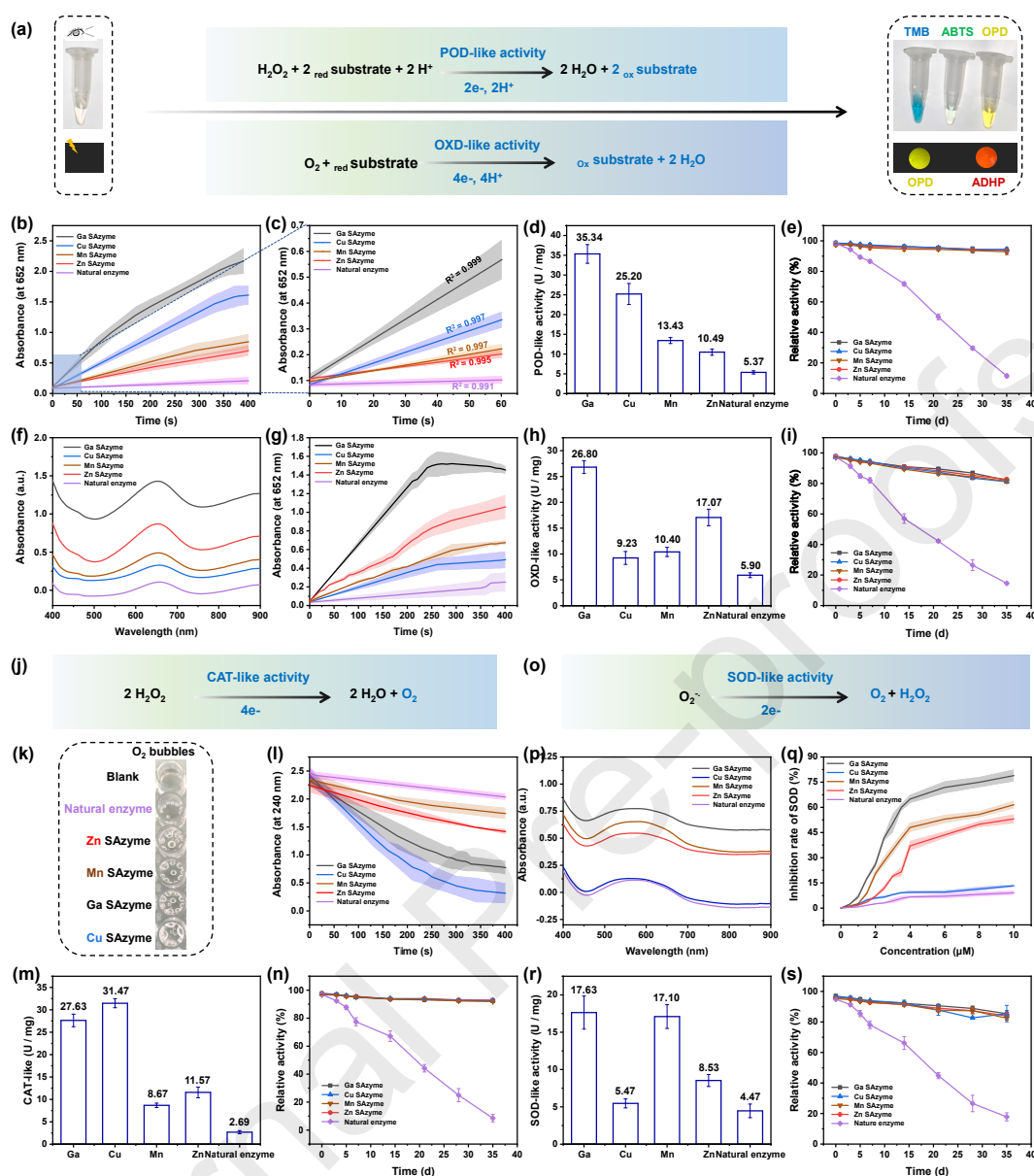3.1. Characterization of Ga, Cu, Mn, and Zn SAzymes
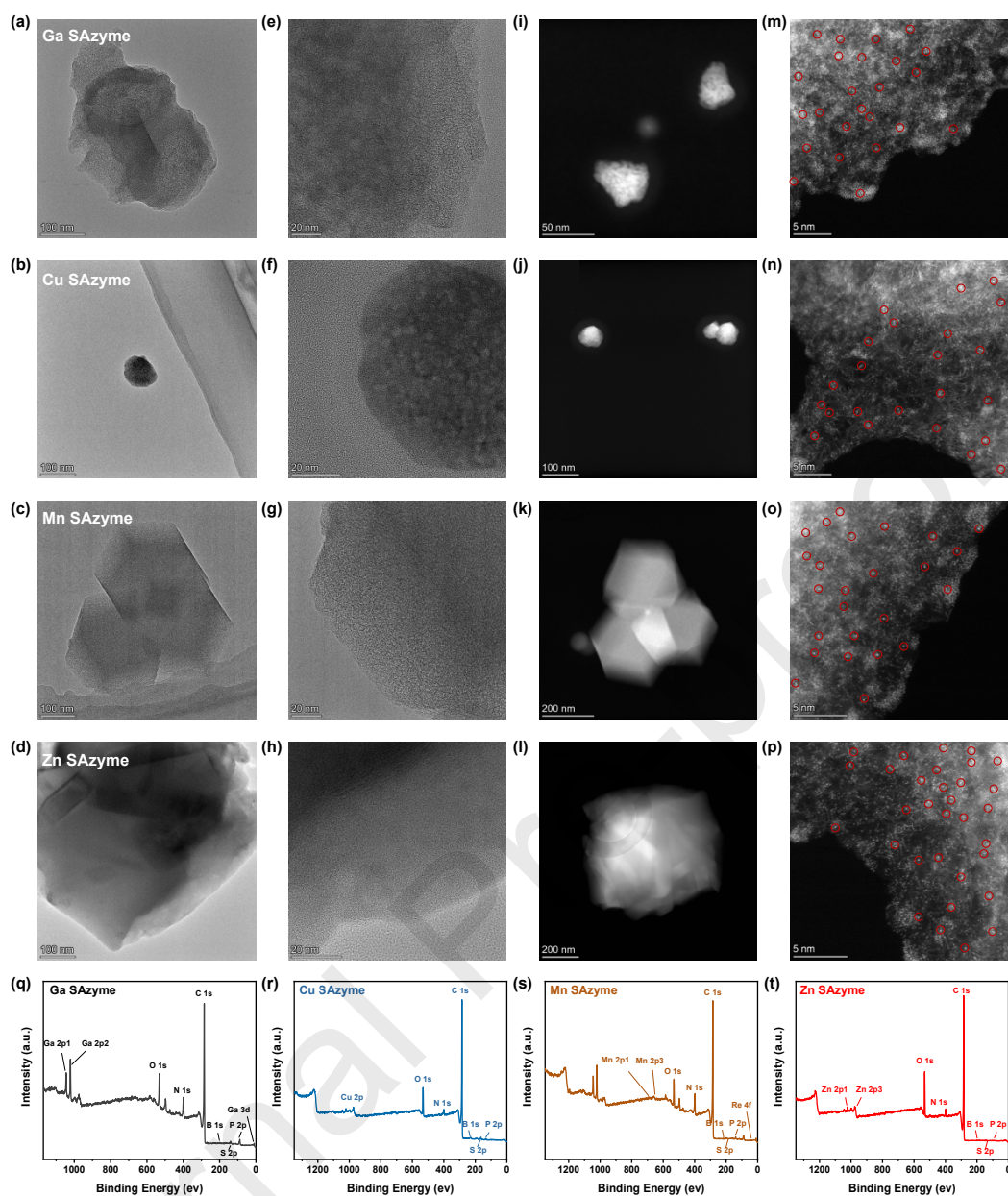
**Fig. 1.** Morphology characterization of Ga, Cu, Mn, and Zn SAzymes. (a-h) TEM images of Ga, Cu, Mn, and Zn SAzymes with the size of 100 nm and 20 nm, respectively. (i-l) AC-HAADF-STEM images of Ga, Cu, Mn, and Zn SAzymes. (m-p) High-resolution AC-HAADF-STEM images of the photo in (i-l), (The red circles highlight single Ga, Cu, Mn, and Zn atoms). (q-t) XPS spectra of Ga, Cu, Mn, and Zn SAzymes.

According to previous research[2, 31, 32], Ga, Cu, Mn, and Zn SAzymes were synthesized using the method of polymer encapsulation. Mn SAzyme preserved the pristine polyhedral structure of zinc-imidazole frameworks (ZIF-8) as observed through transmission electron microscopy (TEM), while Ga, Cu, and Zn SAzymes exhibited an amorphous morphology with abundant micropores (Fig. 1a-h).

7

Additionally, aberration-corrected high-angle annular dark-field scanning transmission electron microscopic (AC-HAADF-STEM) images demonstrated that individual Ga, Cu, Mn, and Zn metal atoms were sparsely dispersed in the nanostructure (Fig. 1i-p). For energy-dispersive Energy dispersive spectrometer (EDS) analysis, single metal atoms and the elements C, N, and O are uniformly distributed throughout the entire nanostructure (Fig. S1). X-ray photoelectron spectroscopy (XPS) identified the presence of major elements (Fig. 1q-t) and nitrogen species such as pyridinic, graphitic, and pyrrolic N, while carbon species were primarily composed of C=O, graphitic C, and C-OH (Fig. S2-6). X-ray diffraction (XRD) spectra showed the absence of metal nanoparticles (Fig. S7). The metal loading of Ga, Cu, Mn, and Zn SAzymes determined by ICP-MS was 3.33 wt%, 3.36 wt%, 3.25 wt%, and 3.43 wt%, respectively.

3.2. Enzyme-like catalytic properties of Ga, Cu, Mn, and Zn SAzymes

**Fig. 2.** The POD-, OXD-, CAT-, and SOD-like catalytic properties of Ga, Cu, Mn, and Zn SAzymes. (a) Catalytic reaction equation of POD-like and OXD-like. (b) Reaction-time curves of the POD-like reaction catalyzed by 3.5 μM Ga, Cu, Mn, Zn SAzymes, and natural enzyme, with the substrate concentration of TMB and $H_2O_2$ at 2.0 mM and 0.5 M, respectively. (c) The corresponding reaction-time curve of the first 60 s in (b). (d) Quantification of specific POD-like catalytic activities and (e) stability analysis. (f) The UV-vis absorption spectra comparison for the OXD-like catalytic activities. (g) Reaction-time curves of the OXD-like reaction catalyzed by 3.5 μM Ga, Cu, Mn, Zn SAzymes, and natural enzyme, with the substrate concentration of TMB at 2.0 mM. (h) Quantification of specific OXD-like catalytic activities and (i) stability analysis. (j) Catalytic reaction equation of CAT-like. (k) Photos show the catalytically generated $O_2$. (l)

9

Reaction-time curves of the CAT-like reaction catalyzed by 3.5 μM Ga, Cu, Mn, Zn SAzymes, and natural enzyme, with the substrate concentration of $H_2O_2$ at 0.5 M. (m) Quantification of specific CAT-like catalytic activities and (n) stability analysis. (o) Catalytic reaction equation of SOD-like. (p) The UV-vis absorption spectra comparison for the SOD-like catalytic activities. (q) Concentration-dependent inhibition rates of Ga, Cu, Mn, Zn SAzymes, and natural enzyme calculated by the NBT colorimetric reaction for SOD-like activities. (r) Quantification of specific SOD-like catalytic activities and stability analysis.
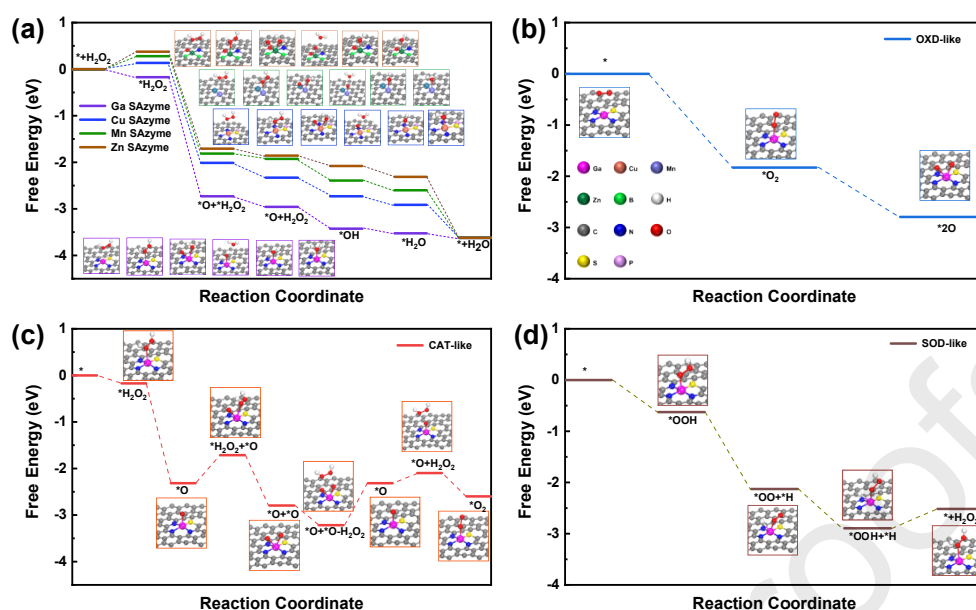
The enzyme-like catalytic properties of Ga, Cu, Mn, and Zn SAzymes were investigated in our research. All four types of SAzymes exhibit POD-like catalytic activity in the presence of $H_2O_2$, resulting in the oxidation of color-developing substrates such as TMB, ABTS, and OPD, as well as fluorescent substrates including OPD and ADHP (Fig. 2a). Among all the oxidation substrates, TMB exhibited the most pronounced color development and stability and was chosen for further experiments. During the reaction time of 0-400 s, the absorbance values at 652 nm was recorded every 10 s. It was observed that Ga SAzyme exhibited superior catalytic properties (Fig. 2b). In the catalytic system within the first 60 s, there was a strong correlation between the catalytic rate of the four types of SAzymes and reaction time (Fig. 2c). The SA value of Ga (35.34 U/mg) was higher than that of Cu (25.20 U/mg), Mn (13.43 U/mg), Zn SAzymes (10.43 U/mg), and the natural enzyme (5.37 U/mg) (Fig. 2d). Additionally, all of them demonstrated high stability (Fig. 2e). Furthermore, the four types of SAzymes were found to catalyze the oxidation of TMB and induced color development even in the absence of $H_2O_2$. They exhibited specific absorption peaks at 652 nm, indicating that all four types of SAzymes possess OXD-like catalytic properties (Fig. 2f). Among them, Ga SAzyme displayed stronger OXD-like catalytic properties (Fig. 2f, g). The SA value of Ga (26.80 U/mg) was higher than that of Zn (17.07 U/mg), Mn (10.40 U/mg), Cu SAzymes (9.23 U/mg), and natural enzyme (5.90 U/mg) (Fig. 2h), and all had high stability (Fig. 2i).

The Ga, Cu, Mn, and Zn SAzymes, as well as natural enzyme showed CAT-like activity and catalyzed the decomposition of $H_2O_2$ into $H_2O$ and $O_2$ bubbles (Fig. 2i, k). During the reaction time from 0 to 400 s, the absorbance values at 240 nm were

10

recorded every 10 s. It was observed that the SA value of Cu (31.47 U/mg) in $H_2O_2$ degradation was higher than that of Ga (27.63 U/mg), Zn (11.57 U/mg), and Mn SAzymes (8.67 U/mg), and all were higher than that of natural enzyme (2.69 U/mg) (Fig. 2l, m). The four types of SAzymes exhibited high stability (Fig. 2n). Scanning the UV-vis absorption spectrum from 400 to 900 nm revealed a distinct absorption peak around 560 nm, which preliminarily confirmed that the four types of SAzymes exhibited SOD-like catalytic activity (Fig. 2o, p). The inhibitory rate was investigated under different amounts of SAzymes additives, and it was found that Ga (17.63 U/mg) mimicked the SOD-like catalytic activity more effectively than Mn (17.10 U/mg), Zn (8.53 U/mg), and Cu SAzymes (5.47 U/mg). They were also stronger than the natural enzyme (4.47 U/mg) (Fig. 2q, r, S8). The four types of SAzymes were more stable than the natural enzyme (Fig. 2s). However, none of the four types of SAzymes exhibited $GP_x$-like (Fig. S9) and PPA-like catalytic activity (Fig. S10).

Furthermore, the four types of SAzymes exhibited optimal reaction pH values and temperature values similar to those of natural enzymes for POD-like and OXD-like activities, which were 4 and 35°C, respectively (Fig. S11, 12). For CAT-like and SOD-like catalytic activities, the optimal reaction pH value and temperature value were 12 and 35°C, respectively (Fig. S13, 14). Then, under the optimal conditions, the enzyme-like activity parameters values (e.g., SA, $K_m$, $v_{max}$, $K_{cat}$, and $K_{cat} / K_m$) were calculated, the results showed that Ga SAzymes exhibited superior catalytic properties compared to others (Fig. S15-18, Table S1-S2).

3.3. Density functional theory (DFT) calculations

**Fig. 3.** Proposed catalytic reaction pathways for enzyme-like activities of Ga, Cu, Mn, and Zn SAzymes. (a) POD-like processes with Ga, Cu, Mn, and Zn SAzymes. (b) OXD-like process, (c) CAT-like process, and (d) SOD-like processes with Ga SAzyme (Illustration is the chemical structure formula of each stage).

The differences in the catalytic properties of four single-atom nanozymes were explored with the same synthesis method and comparable metal loading. To explore the underlying reaction mechanism and provide support for the high POD-like catalytic efficiency, a range of intermediate / transition states of Ga, Cu, Mn, and Zn SAzymes attached to various chemical units using density functional theory (DFT). The simulated catalytic pathways are summarized in Fig. 3a. Previous theoretical studies[33, 34] have identified the hydroxyl-adsorbed structure as a key intermediate, and the adsorption energy of hydroxyl ($E_{ads}$, OH) can serve as a descriptor for the catalytic property of POD-like SAzymes. The POD activity window, as defined by $E_{ads}$, OH was -3.5 to -1.6 eV. The DFT calculated $E_{ads}$, OH suggests that the Ga site is more favorable than the other three single-atom sites, as its $E_{ads}$, OH (-3.43 eV) falls within a closer range of values compared to the other three (-2.73 eV, -2.39 eV, and -2.08 eV) for Cu, Mn, and Zn SAzymes, respectively (Table S2). These results indicate that the presence of Ga sites can significantly enhance the POD-like activity, which is consistent with our previous research results (Fig. 2d). Compared to the POD-like

processes, the simulated OXD-, CAT-, and SOD-like processes are generally less complex, as shown in Fig. 3b-d. The high OXD-, CAT-, and SOD-like catalytic activities of Ga SAzyme were quantitatively calculated to be 26.80 U/mol, 27.63 U/mol, and 17.63 U/mol (Fig. 2), respectively. And these activities can be attributed to the low energy barriers predicted by DFT simulations (Table S3).

3.4. Validation of the species and contents of intermediate
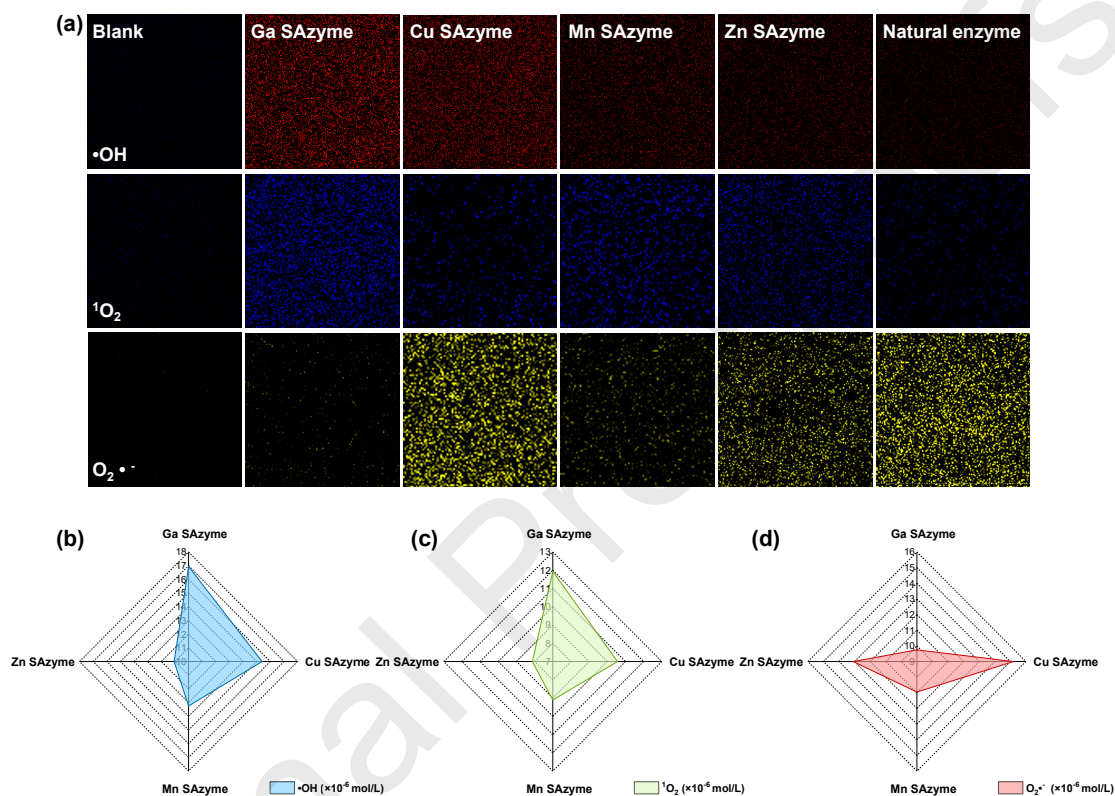


**Fig. 4.** Comparison of redox intermediate types and contents. (a) Capture of specific intermediates (confocal photography). Quantitative content comparison of (b) •OH, (c) $^1O_2$, and (d) $O_2$•$^-$ for Ga, Cu, Mn, and Zn SAzymes.

In the process of redox reactions, the generation of intermediates (e.g., •OH, $^1O_2$, and $O_2$•$^-$) are accompanied. By selectively capturing and quantifying the types and amounts of intermediates produced by Ga, Cu, Mn, and Zn SAzymes, we can indirectly compare their enzyme-like catalytic activities. The results are depicted in Fig. 4a. Compared with natural enzymes, all four SAzymes exhibited the generation of three reactive oxygen intermediates within 10 min. Moreover, Ga SAzyme produced higher levels of •OH and $^1O_2$ during the catalytic reaction process, which

can be attributed to the electron transfer rate at the gallium surface[32, 35]. Qualitative and quantitative analysis of the intermediate contents in each system were further conducted using EPR. The analysis revealed that all four types of SAzymes produced higher levels of intermediate contents at 10 min (Fig. S19). It is evident that Ga SAzyme demonstrates stronger enzyme-like catalytic activity compared to the other three SAzymes (Fig. 4b-d), which are consistent with the above research findings (Fig. 2).

## 3.5. Application the optimal single-atom nanozyme for ammonia response
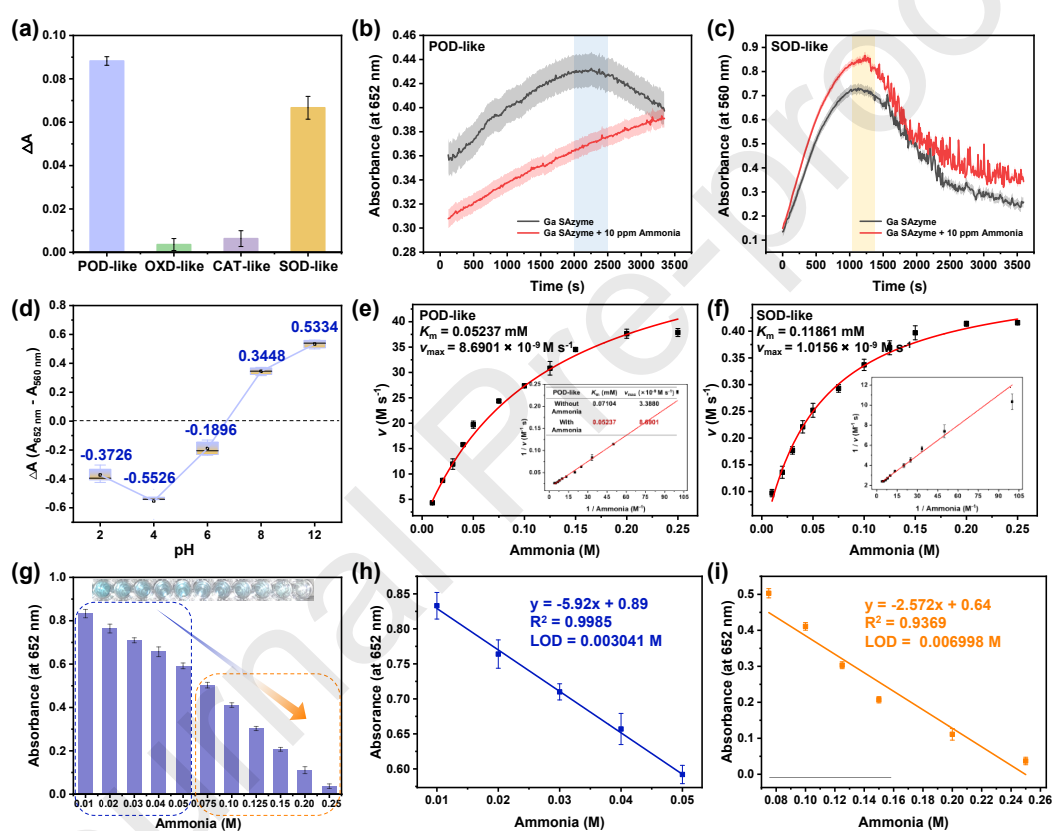


**Fig. 5.** Effect of ammonia on enzyme-like catalytic performance of Ga SAzyme. (a) Changes in absorbance of systems with and without ammonia. Reaction-time curves of (b) POD-like and (c) SOD-like reaction catalyzed by 3.5 μM Ga SAzyme at an ammonia concentration of 10 ppm. (d) Comparison of the absorbance of POD-like and SOD-like catalytic activities of Ga SAzyme at different pH values. Affinity of (e) POD-like and (f) SOD-like activity of Ga SAzyme to ammonia. (g) Sensitivity response of POD-like catalytic activity of Ga SAzyme to ammonia. Linear regression curve between ammonia concentration and absorbance value at 652 nm in the linear range of (h) 0.01 - 0.05 M and (i) 0.075 - 0.25 M. LOD = 3σ / k (The σ value denotes the

standard error of the results from 20 blank sample determinations, and the k value is the slope of the linear fit equation)

We further explored the response performance of Ga SAzyme towards ammonia. The 10 μL of 10 ppm ammonia was added to four types of enzyme-like catalytic systems of Ga SAzyme (e.g., POD-, OXD-, CAT-, and SOD-like). It was found that ammonia had a significant impact on the POD-like and SOD-like catalytic activities of Ga SAzyme (Fig. 5a, S20). Over time, the decrease in POD-like catalytic activity caused by ammonia was more significant than the increase in SOD-like catalytic activity (Fig. 5b, c, Fig. S21). Furthermore, under different pH values catalytic conditions, the POD-like catalytic activity showed the most significant variation as the pH value increased (Fig. 5d). Additionally, the affinity of the POD-like system for ammonia ($K_m = 0.05$ mM) was found to be stronger than that of the SOD-like system ($K_m = 0.12$ mM), and TMB ($K_m = 0.07$ mM) (Fig. 5e, f). In our study, these results indicate that the POD-like catalytic activity of Ga SAzyme is most sensitive to changes in pH value. Based on this, the sensitivity of the POD-like catalytic activity of Ga SAzyme was utilized for the detection of VAGs, specifically ammonia (Fig. 5g-i). Within the linear range of 0.01 - 0.05 M, the limit of detection (LOD) for ammonia was 3.0 mM. In the linear range of 0.075 - 0.25 M, the LOD was 7.0 mM. Compared to previous research results (Table S4), the LOD of Ga SAzyme for VAGs is lower, which makes it very promising for future practical detection applications. I In addition, similar results were obtained after seven repetitions under the same experimental operating conditions, indicating that the Ga SAzyme sensor has good reproducibility (Fig. S22a). Meanwhile, the Ga SAzyme sensor also showed good response performance to other VAGs (e.g., dimethylamine and trimethylamine), but did not show any signal change in response to non-VAGs (e.g., $N_2$, $CO_2$, $H_2O$, $O_2$, and $H_2S$). This shows that the Ga SAzyme sensor has good selectivity for total VAGs in the presence of interfering substances (Fig. S22b).

## 4. Conclusion and prospect

The type of metal atom in SAzymes plays a crucial role in their catalytic activity. This study systematically analyzed the multienzyme-like types and catalytic activities

of four different metal species (Ga, Cu, Mn, and Zn SAzyme). It was found that all four types of SAzyme exhibited POD-, OXD-, CAT-, and SOD-like catalytic activities. A comprehensive comparison revealed that Ga SAzyme demonstrated superior enzyme-like catalytic properties, which can be attributed to its high electron transfer efficiency on the surface. Further, the impact of VAGs, specifically ammonia, on the multienzyme-like catalytic properties of Ga SAzyme was investigated. The presence of ammonia significantly impacted the POD-like and SOD-like catalytic activities, with the POD-like system showing a stronger affinity for ammonia ($K_m$ = 0.05 mM) compared to the SOD-like system ($K_m$ = 0.12 mM). It can be used Ga SAzyme to achieve a highly sensitive detection to ammonia, and the entire process does not require complicated procedures, expensive reagents, and equipment. The LOD is 3.0 mM within the linear range of 0.01 - 0.05 M, and the LOD is 7.0 mM in the linear range of 0.075 - 0.25 M. The response time is approximately 15 s and the cost is approximately \$0.035 per sample (Table S6). Compared to previous research, the VAGs detection method developed in this study offers lower detection limits, faster response times, and reduced costs. It is expected to be used for detecting VAGs in the fields of food and environmental monitoring in the future.

**CRediT authorship contribution statement**

**Guangchun Song:** Methodology, Investigation, Formal analysis, Data curation, Writing-original draft. **Xiaochun Zheng:** Conceptualization, Supervision, Validation, Writing-review & editing. **Zedong Zhang:** Conceptualization, Validation, Writing-review & editing. **Marie-Laure Fauconnier:** Investigation, Formal analysis. **Cheng Li:** Writing-review & editing. **Li Chen:** Conceptualization, Supervision, Writing-review & editing. **Dequan Zhang:** Supervision, Validation, Writing-review & editing, Funding acquisition.

**Declaration of Competing Interest**

The authors declare that they have no known competing financial interests or personal relationships that could have appeared to influence the work reported in this paper.

**Acknowledgements**

**Appendix A. Supporting data**

Supporting Information is available from the author.

**Data availability**

Data will be made available on request.

**Reference**

[1] BEKHIT E D A, HOLMAN B W B, GITERU S G, et al. Total volatile basic nitrogen (TVB-N) and its role in meat spoilage: A review [J]. Trends in Food Science & Technology, 2021, 109: 280-302.

[2] SONG G, ZHANG Z, FAUCONNIER M-L, et al. Bimodal single-atom iron nanozyme biosensor for volatile amine and food freshness detection [J]. Nano Today, 2023, 53: 102025-34.

[3] ZHAO J, NI Y, TAN L, et al. Recent advances in meat freshness "magnifier": fluorescence sensing [J]. Critical reviews in food science and nutrition, 2023, 1-17.

[4] DEVAULL G E. Improved exposure estimation in soil screening and cleanup criteria for volatile organic chemicals [J]. Integrated environmental assessment and management, 2017, 13(5): 861-9.

[5] ASIF Z, CHEN Z, HAGHIGHAT F, et al. Estimation of Anthropogenic VOCs Emission Based on Volatile Chemical Products: A Canadian Perspective [J]. Environmental management, 2023, 71(4): 685-703.

[6] PAWAR D, KANAWADE R, KUMAR A, et al. High-Performance Dual Cavity-Interferometric Volatile Gas Sensor Utilizing Graphene/PMMA Nanocomposite [J]. Sensors and Actuators B Chemical, 2020, 312(1): 127921.

[7] CHEN Y, OWYEUNG R E, SONKUSALE S R. Combined optical and electronic paper-nose for detection of volatile gases [J]. Analytica Chimica Acta 2018, 1034: 128-36.

[8] KESSELMEIER J, STAUDT M J. Biogenic Volatile Organic Compounds (VOC): An Overview on Emission, Physiology and Ecology [J]. Journal of Atmospheric Chemistry, 1999, 33(1): 23-88.

[9] WITKOWSKA D. Volatile gas concentrations in turkey houses estimated by Fourier Transform Infrared Spectroscopy (FTIR) [J]. British poultry science, 2013, 54(3): 289-97.

[10] HONOUR J W. Gas chromatography-mass spectrometry [J]. Methods in molecular biology (Clifton, NJ), 2006, 324: 53-74.

[11] BARTOSZ S, JACEK G B. Currently Commercially Available Chemical Sensors Employed for Detection of Volatile Organic Compounds in Outdoor and Indoor Air [J]. Environments, 2017, 4(1): 21.

[12] MOON H G, JUNG Y, HAN S D, et al. Chemiresistive Electronic Nose toward Detection of Biomarkers in Exhaled Breath [J]. ACS Applied Materials & Interfaces, 2016, 8(32): 20969-76.

[13] ZHAO G, DONG X, DU Y, et al. Enhancing Electrochemiluminescence Efficiency through Introducing Atomically Dispersed Ruthenium in Nickel-Based Metal-Organic Frameworks [J]. Analytical chemistry, 2022, 94(29): 10557-66.

[14] WANG Y, ZHAO G, CHI H, et al. Self-Luminescent Lanthanide Metal-Organic Frameworks as Signal Probes in Electrochemiluminescence Immunoassay [J]. Journal of the American Chemical Society, 2020, 143(1): 504-12.

[15] ZHANG S, LI Y, SUN S, et al. Single-atom nanozymes catalytically surpassing naturally occurring enzymes as sustained stitching for brain trauma [J]. Nature Communications 2022, 13(1): 4744-60.

[16] LI Z, LIU F, CHEN C. Regulating the N Coordination Environment of Co Single-Atom Nanozymes for Highly Efficient Oxidase Mimics [J]. Nano Letters 2023, 23(4): 1505-13.

[17] CHEN Y, JIANG B, HAO H, et al. Atomic-Level Regulation of Cobalt Single-Atom Nanozymes: Engineering High-Efficiency Catalase Mimics [J]. Angewandte Chemie International Edition, 2023, 62(19): e202301879-e88.

[18] LIU C, GUI L, ZHENG J J. Intrinsic Strain-Mediated Ultrathin Ceria Nanoantioxidant [J]. Journal of the American Chemical Society, 2023, 145(34): 19086-97.

[19] MUHAMMAD P, HANIF S, LI J. Carbon dots supported single Fe atom nanozyme for drug-resistant glioblastoma therapy by activating autophagy-lysosome pathway [J]. Nano Today, 2022, 45: 101530-47.

[20] SONG G, LI J C, MAJID Z, et al. Phosphatase-like activity of single-atom CeNC nanozyme for rapid detection of Al(3) [J]. Food chemistry, 2022, 390(1):

133127-34.

[21] CHENG C, WANG H, ZHAO J, et al. Advances in the application of metal oxide nanozymes in tumor detection and treatment [J]. Colloids and Surfaces, B Biointerfaces, 2024, 235: 113767-75.

[22] HU C, HOU B, YANG F, et al. Enhancing diabetic wound healing through anti-bacterial and promoting angiogenesis using dual-functional slow-release microspheres-loaded dermal scaffolds [J]. Colloids and surfaces B, Biointerfaces, 2024, 242: 114095-108.

[23] SONG G, ZHANG J, HUANG H, et al. Single-atom Ce-N-C nanozyme bioactive paper with a 3D-printed platform for rapid detection of organophosphorus and carbamate pesticide residues [J]. Food chemistry, 2022, 387: 132896-905.

[24] SONG G, ZHANG Q, LIANG S, et al. Oxidation activity modulation of a single atom Ce-N-C nanozyme enabling a time-resolved sensor to detect $Fe^{3+}$ and $Cr^{6+}$ [J]. Journal of Materials Chemistry C, 2022, 10(41): 15656-63.

[25] CAI X, MA F, JIANG J, et al. Fe-N-C single-atom nanozyme for ultrasensitive, on-site and multiplex detection of mycotoxins using lateral flow immunoassay [J]. Journal of Hazardous Materials, 2023, 441(5): 129853-15.

[26] LIU Q, ZHU X, ZHONG L, et al. Recent advances in the applications of nanozymes for the efficient detection/removal of organic pollutants: a review [J]. Environmental Science: Nano, 2022, 9(4): 1212-35.

[27] SUN H, CAI S, WANG C, et al. Recent Progress of Nanozymes in the Detection of Pathogenic Microorganisms [J]. ChemBioChem, 2020, 21(18): 2572-84.

[28] ZONG B, XU Q, MAO S. Single-Atom Pt-Functionalized $Ti_3C_2T_x$ Field-Effect Transistor for Volatile Organic Compound Gas Detection [J]. ACS Sensors, 2022, 7(7): 1874-82.

[29] SHEN L, YE D. Perspectives for Single-Atom Nanozymes: Advanced Synthesis, Functional Mechanisms, and Biomedical Applications [J]. Analytical Chemistry, 2021, 93(3): 1221-31.

[30] ZHAO X, WANG F, KONG X P, et al. Dual-Metal Hetero-Single-Atoms with

Different Coordination for Efficient Synergistic Catalysis [J]. Journal of the American Chemical Society, 2021, 143(39): 16068-77.

[31] ZEDONG ZHANG J Z, SHENGHUA CHEN, WENMING SUN, AND DINGSHENG WANG. Liquid Fluxional Ga Single Atom Catalysts for Efficient Electrochemical $CO_2$ Reduction [J]. Angewandte Chemie International Edition 2023, 62(3): e202215136-e44.

[32] ZHANG Z, ZHU J, CHEN S, et al. Liquid Fluxional Ga Single Atom Catalysts for Efficient Electrochemical $CO_2$ Reduction [J]. Angewandte Chemie International Edition, 2023, 62(3): e202215136.

[33] SHEN X, WANG Z, GAO X, et al. A Density Functional Theory-Based Method to Predict the Activities of Nanomaterials as Peroxidase Mimics [J]. ACS Catalysis, 2020, 10(21): 12657-65.

[34] MA C B, XU Y, WU L, et al. Guided Synthesis of a Mo/Zn Dual Single-Atom Nanozyme with Synergistic Effect and Peroxidase-like Activity [J]. Angewandte Chemie International Edition 2022, 61(25): e202116170-e80.

[35] HSIEH T E, FRISCH J, WILKS R G. Unravelling the Surface Oxidation-Induced Evolution of the Electronic Structure of Gallium [J]. ACS Applied Materials & Interfaces, 2023, 15(40): 47725-32.

**Highlights**

- A computational and screening approach offered for evaluating enzyme-like catalytic properties of SAzymes.
- The POD-like activity of Ga SAzyme is most sensitive by changes in pH values than others.
- A stronger affinity for ammonia ($K_m$ = 0.05 mM) compared to TMB ($K_m$ = 0.07 mM) of Ga SAzyme.
- A sensitive (LOD is 3.0 mM), rapid (15 s), and cost-effective ($0.035 per sample) method was developed for VAGs detection.